Effect of humic acid on the adsorption/desorption behavior of glyphosate on goethite. Isotherms and kinetics

Jeison Manuel Arroyave, Carolina C. Waiman, Graciela P. Zanini, Marcelo J. Avena[*]

INQUISUR, Department of Chemistry, Universidad Nacional del Sur, Av. Alem 1253, B8000CPB, Bahía Blanca, Argentina

HIGHLIGHTS

- Attachment of glyphosate to goethite particles is inhibited by humic acid.
- Adsorbed humic acid decreases the adsorption rate of glyphosate.
- Humic acid in solution increases the desorption rate.
- Glyphosate desorbs by two parallel processes.

GRAPHICAL ABSTRACT
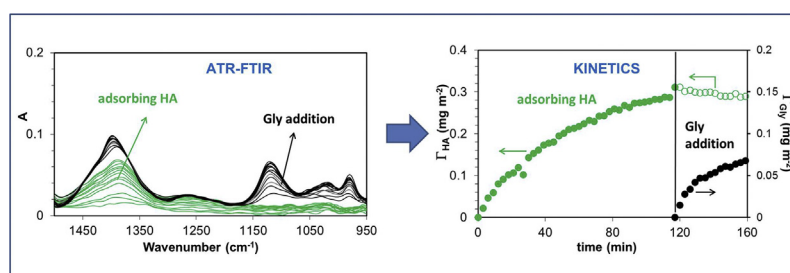
ABSTRACT

The effects of humic acid (HA) on the adsorption/desorption of glyphosate (Gly) on goethite were investigated under pseudo equilibrium conditions by adsorption isotherms and under kinetic conditions by ATR-FTIR spectroscopy. Isotherms reveal that the attachment of Gly is almost completely inhibited by HA molecules. The opposite effect is not observed: HA adsorption is not affected by the presence of Gly. ATR-FTIR allowed the simultaneous detection of adsorbed HA and Gly during kinetic runs, revealing that HA at the surface decreases markedly the adsorption rate of Gly likely as a result of a decreased availability of sites for Gly adsorption and because of electrostatic repulsion. In addition, HA in solution increases the desorption rate of Gly. The rate law for Gly desorption could be determined giving important insights on the desorption mechanism. The herbicide is desorbed by two parallel processes: i) a direct detachment from the surface, which is first order in adsorbed Gly; and ii) a ligand exchange with HA molecules, which is first order in adsorbed Gly and first order in dissolved HA. Rate constants for both processes were quantified, leading to half-lives of 3.7 h for the first process, and 1.4 h for the second process in a 400 mg L^{-1} HA solution. These data are important for modeling the dynamics of glyphosate in environmentally relevant systems, such as soils and surface waters.

1. Introduction

Glyphosate (Gly) is a broad-spectrum organophosphorus herbicide widely used in agriculture and horticulture (Aparicio et al., 2013; Yang et al., 2015). It is the most used herbicide in the world. Recently, the International Agency for Research on Cancer (IARC) of the World Health Organization (WHO) has classified Gly as probably carcinogenic to humans (Group 2A) because there is convincing evidence that it can cause cancer in laboratory animals (Guytona et al., 2015). It was also reported that it has some immunotoxic effects on fish (Ma and Li, 2015). Studying the

---

* Corresponding author. INQUISUR, Departamento de Química, Universidad Nacional del Sur, Av. Alem 1253, B8000CPB, Bahía Blanca, Argentina.
E-mail address: mavena@uns.edu.ar (M.J. Avena).

processes that affect the mobility and distribution of Gly in natural systems, such as soils and surface waters, is therefore of crucial importance to understand its behavior and fate in the environment.

The mobility of Gly in the environment is strongly influenced by adsorption/desorption processes on mineral surfaces, especially on hydrous ferric oxides surfaces, which bear high affinity for it. The adsorption of Gly on hydrous ferric oxides has been investigated in several studies (Barja and dos Santos Afonso, 2005; Gimsing and Borggaard, 2001, 2002) and takes place mainly by a ligand exchange mechanism, resulting in the formation of inner-sphere surface complexes, where the phosphonate group of Gly binds Fe(III) ions at the surface displacing coordinated water molecules and/or hydroxyl ions (Sheals et al., 2002). It is also well-known that the adsorption of Gly is affected by the presence of other adsorbing species, particularly those species that are also capable of forming complexes with Fe(III) ions at the surface. This is the case of phosphate, which is a good ligand and thus can displace Gly from adsorption sites by ligand exchange (Waiman et al., 2013). It should be also the case of humic substances, such as humic acids (HAs) or fulvic acids (FAs) (Tipping, 1994; Antelo et al., 2007; Fu and Quan, 2006; Weng et al., 2006), which have carboxylate groups in their structure, with the potential ability to affect Gly adsorption/desorption processes. The effects of phosphate on the adsorption behavior of Gly on metal oxides have been reported in several articles (Gimsing and Borggaard, 2001, 2002; Waiman et al., 2013). Conversely, the effects of humic substances were seldom investigated. In this respect, Day et al. (1997) informed that the natural organic matter obtained from a stream in Victoria, Australia, decreased the adsorption of Gly on goethite (α-FeOOH), likely because of competition for surface sites and by electrostatic and perhaps steric shielding effects. This seems to be the only report in the literature regarding HA effects on Gly adsorption/desorption kinetics, and thus more information is still needed.

The aim of this paper is to study the effects of HA on the adsorption/desorption behavior of glyphosate on goethite. Adsorption isotherms in batch experiments are performed and adsorption/desorption kinetic studies using Attenuated Total Reflectance Fourier Transform Infrared Spectroscopy (ATR-FTIR) are reported. Emphasis is given in Gly desorption, aiming to investigate the influences of HA on its desorption rate, to asses a rate law for the desorption process, and to show the capabilities of ATR-FTIR to obtain kinetic information of environmentally relevant systems.

2. Experimental

2.1. Goethite and HA

Goethite particles were synthesized as described by Puccia et al. (2009), following the methodology proposed by Atkinson et al. (1967). A 5 M NaOH solution was added dropwise (10 mL min^{-1}) to a stirred 0.1 M Fe(NO$_3$)$_3$·9H$_2$O aqueous solution until the pH was 12. N$_2$ was continuously bubbled in the reaction vessel during the NaOH addition to reduce CO$_2$ contamination. The resulting suspension was aged at 60 °C for 3 days in a capped teflon container in order to produce goethite crystallization. The suspension was then filtered and the solid particles were washed with CO$_2$-free water until the conductivity of the supernatant was lower than 10 μS cm^{-1}. The washed solid was finally stored as a stock suspension at pH 4.5. It had a N$_2$-BET surface area of 89.7 m^2 g^{-1}, a pore volume of 0.36 cm^3 g^{-1} and a pore size of 16 nm. Its isoelectric point (IEP) was 8.6 in aqueous NaCl solutions.

The HA was extracted from an alfalfa-cultivated soil (INTA, Manfredi Experimental Station, Córdoba, Argentina) and purified according to the procedures recommended by the IHSS (International Humic Substances Society) (Swift, 1996). The HA sample has

an elemental composition of C (54.4%), H (4.0%), N (1.6%), and O (39.9%), and an ash content of 1.18%. More information about the general characteristics of this HA sample can be found elsewhere (Sola et al., 1988).

2.2. Gly and HA adsorption isotherms

Gly (pKa: <2, 2.12, 7.21 and 12.32) and HA adsorption isotherms were obtained by batch equilibration experiments. They were performed by adding 0.7 mL of the stock goethite suspension (9.63 g L^{-1}) to 15 mL polypropylene centrifuge tubes containing 10 mL of an aqueous solution of known concentration of Gly or HA. The background electrolyte was 0.1 M NaCl. The pH of these dispersions was adjusted to 7.0 and kept constant by adding a few microliters of either NaOH or HCl solutions. The tubes were shaken for 6 h with an end-over-end rotator and the final pH was always in the range 7.0 ± 0.1. Finally, the supernatants were separated by centrifugation and used for quantification of Gly or HA that remained in solution.

The effect of HA on the adsorption of Gly was investigated by performing Gly adsorption isotherms to goethite samples that were subjected first to HA adsorption. 0.7 mL of the stock goethite suspension were added to 15 mL polypropylene centrifuge tubes containing 10 mL of an aqueous solution of the desired HA concentration. The pH was adjusted and the suspensions were shaken for 6 h to produce the HA adsorption. Once HA was adsorbed on the goethite particles, Gly solutions of increasing concentrations were added to the tubes, the pH was readjusted if necessary, and the resulting suspensions were shaken again for 6 h. The supernatants were then separated by centrifugation and used for quantification of Gly and HA. All experiments were done at pH 7.0 in 0.1 M NaCl, where Gly and HA are in their anionic forms.

The concentration of Gly in the supernatant was measured by UV–vis spectrophotometry after a derivatization step with FMOC-Cl (fluorenylmethyloxycarbonyl chloride) in alkaline media. A full description of the method can be found elsewhere (Waiman et al., 2012). The spectra were recorded in the 200–900 nm wavelength range and the absorbance at 265 nm was used for quantification. The concentration of HA in the supernatant was also measured by UV–vis spectroscopy. The spectra were recorded and the HA concentration was then evaluated from the absorbance at 500 nm. In both cases, calibration curves were constructed with Gly and HA solutions prepared at pH 7.0 in 0.1 M NaCl. An Agilent 8453 UV–Vis diode array spectrophotometer equipped with a Hellma 1-cm quartz cell was used for absorbance readings.

2.3. ATR-FTIR measurements

ATR-FTIR spectra were acquired with a Nicolet Nexus 470 FTIR spectrometer equipped with a DTGS detector, a SMART-ARK ATR accessory and a ZnSe crystal (area: 10 × 72 mm, incident angle: 45°, total reflections: 12, trough cell). A film of goethite particles was prepared on the ZnSe crystal by placing 210 μL of the 9.63 g L^{-1} goethite stock suspension on the crystal and evaporating to dryness at room temperature. The so-prepared film was covered with 1 mL of a 0.1 M NaCl solution and a blank spectrum was recorded. The NaCl solution was then replaced by either a HA or a Gly solution of the desired concentration and spectra were recorded as a function of time. Each spectrum is the result of the average of 256 scans, with a spectral resolution of 4 cm^{-1}. The time needed to collect each spectrum was 3 min. Gly and HA solutions were always prepared at pH 7.0 and in 0.1 M NaCl.

ATR-FTIR spectroscopy was used to perform two main types of experiments in order to investigate the effects of HA on Gly adsorption and desorption. They are described below.

2.3.1. Gly adsorption on HA-containing goethite

In these experiments HA was adsorbed first, and a Gly solution was added afterwards. The aim was to evaluate the effect of previously adsorbed HA on Gly adsorption. Three different HA loadings were explored: 0.32, 0.62 and 1.25 mg m^{-2}. The goethite film was prepared as described above, and then a HA solution was added to achieve the desired loading. Spectra were collected during this procedure. Once HA was adsorbed, the solution in contact with the goethite film was replaced with a 16.9 mg L^{-1} (10^{-4} M) Gly solution and new spectra were recorded as a function of time. It is difficult to keep a perfect control of pH in ATR-FTIR experiments since the volume of the solution on top of the goethite film was around 1 mL. In spite of this, in some of these and the following experiments the pH was measured with a surface electrode and it was always between 7.0 and 7.5.

2.3.2. Gly desorption by addition of HA

In these experiments Gly was adsorbed first, and HA was added afterwards at different concentrations. The aim was to evaluate if the addition of HA produced desorption of a previously adsorbed Gly. Once the goethite film was prepared, Gly was adsorbed by adding 1 mL of a 16.9 mg L^{-1} (10^{-4} M) Gly solution. The ATR-FTIR spectra corresponding to Gly adsorption were then collected as a function of time. Afterwards, the solution in contact with the goethite film was replaced with HA solutions of 0, 50, 116 and 233 mg L^{-1} and new spectra were recorded as a function of time.

2.4. Theoretical background

The ATR-FTIR quantification of adsorbed Gly and HA can be accessed from the spectral information obtained in systems containing both adsorbed substances. In these systems, the absorbance in the IR is proportional to the amount of the IR-active species (Waiman et al., 2013; Roncaroli and Blesa, 2011), which in our case are adsorbed Gly and HA. Their quantification in a mixture can be achieved by working at two different wavenumbers, using a system of equations that is very similar to that used to quantify spectrophotometrically a mixture of two dissolved species by UV—Vis at two different wavelengths. In the case of IR, the total absorbance, A_T, at each wavenumber is equal to the sum of the individual absorbance of Gly, A_{Gly}, and the individual absorbance of HA, A_{HA}.

$$A_T = A_{HA} + A_{Gly} \qquad (1)$$

Therefore, by analyzing data at two different wavenumbers, 1 and 2, the two equations to solve are:

$$A_T^1 = \kappa_{HA}^1 \Gamma_{HA} + \kappa_{Gly}^1 \Gamma_{Gly} \qquad (2)$$

$$A_T^2 = \kappa_{HA}^2 \Gamma_{HA} + \kappa_{Gly}^2 \Gamma_{Gly} \qquad (3)$$

where κ_{HA} and κ_{Gly} are proportionality constants and Γ_{HA} and Γ_{Gly} are the adsorbed amounts of HA and Gly respectively. The superscripts 1 and 2 denote the two different wavenumbers at which the absorbance values are analyzed. The values of κ_{HA}^1 and κ_{HA}^2 can be known from measurements with HA alone, and the values of κ_{Gly}^1 and κ_{Gly}^2 can be known from measurements with Gly alone. Thus, the two-equations system can be solved and the two unknowns Γ_{HA} and Γ_{Gly} can be calculated from the spectra.

3. Results and discussion

3.1. Gly and HA adsorption isotherms

The adsorption isotherms of Gly and HA are shown in Fig. 1. Gly adsorption increases up to a maximum of 0.21 mg m^{-2}, which is a value normally found in the literature (Barja and dos Santos Afonso, 2005; Sheals et al., 2002). This maximum is reached at Gly concentrations of around 4×10^{-5} M. Considering that Gly is normally applied in farms in formulations with a concentration of around 4×10^{-2} M (Candela et al., 2010), the formulation concentration is three orders of magnitude higher than the needed to saturate the goethite surface, indicating that high surface coverages could be achieved in the upper part of the soil. The adsorption of HA under the same conditions is around six times higher, reaching a maximum of 1.25 mg m^{-2}, which is also a normal value for HA adsorption on goethite (Antelo et al., 2007). The HA isotherm looks
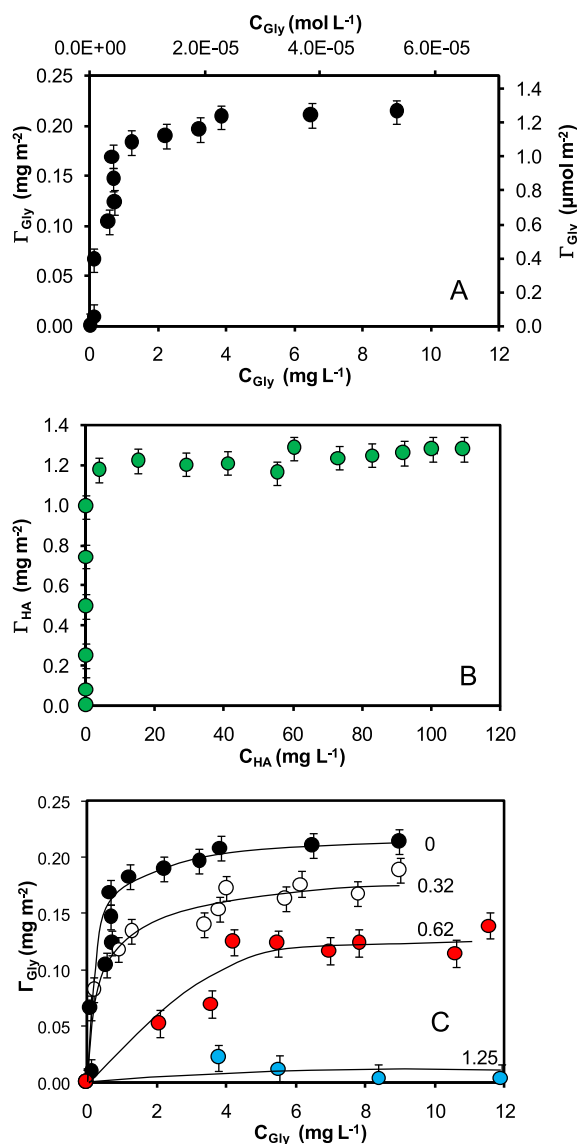

Fig. 1. A) Adsorption isotherm of Gly on goethite; B) adsorption isotherm of HA on goethite; C) adsorption isotherms of Gly on goethite containing different amounts of adsorbed HA, the respective values of Γ_{HA} in mg m^{-2} are given close to each isotherm. Error bars indicate standard deviation. pH 7.0 and 0.1 M NaCl in all cases. c$_{Gly}$ and c$_{HA}$ are Gly concentration and HA concentration respectively.

like a high affinity isotherm, with all points laying on the y-axis until surface saturation is reached. In fact, no HA could be detected in the supernatant solution before this saturation was attained, meaning that all added HA was adsorbed by the solid.

Fig. 1C shows adsorption isotherms of Gly on goethite containing different amounts of adsorbed HA. It must be remarked that no HA could be detected in the supernatant solutions after the reaction, indicating that all HA remained adsorbed on the particles. The presence of HA has an important effect on the adsorption of Gly, which decreases as adsorbed HA increases. For the highest HA content the effect was so strong that there was only a very low adsorption of Gly. According to Day et al. (1997), HA affects the adsorption of Gly because HA binds the goethite surface occupying adsorption sites and impeding the adsorption of the herbicide. They also indicate that electrostatic repulsion between adsorbed HA and adsorbing Gly, and steric effects caused by adsorbed HA would also prevent Gly adsorption. This effect of adsorbed HA on the subsequent adsorption of an anionic herbicide has been observed for similar systems. For example, Celis et al. (1999) found that HA coatings reduced the adsorption of the anionic herbicide 2,4-D by montmorillonite-iron oxide binary systems. Although HA decreases markedly the adsorption of Gly, there is no indication of a similar effect of Gly on HA adsorption. As indicated above, all added HA remained adsorbed on the particles irrespective of the amount of Gly present in the system.

3.2. ATR-FTIR measurements

The ATR-FTIR spectra of Gly and HA adsorbed on goethite are shown in Fig. 2. Data analysis is focused in the $900-1700$ cm^{-1} region, where IR bands appear for both compounds. IR absorption bands of adsorbed Gly are located at 1585, 1400, 1322, 1120, 1016 and 980 cm^{-1}. The band centered around 1585 cm^{-1} usually appears with some spectral artifacts between 1610 and 1670 cm^{-1} because of the strong IR absorption of water (solvent). Gly absorption bands correspond to the $\nu_a(C-O)$, $\nu_s(C-O)$, $\nu(C-O-P)$, $\nu_a(P-O)$, $\nu_a(P-OFe)$ and $\nu_s(P-OFe)$ vibration modes respectively. According to Sheals et al. (2002), these vibrations are characteristic of a monodentate mononuclear inner-sphere complex, in which the phosphonate group of Gly is bonded to a Fe (III) center of the goethite surface. Even though carboxylate can act as a ligand, the experimental evidence by IR and XPS (Sheals et al., 2002) indicates that only the phosphonate group is directly bonded to the goethite surface, whereas carboxylate remains relatively "free" form complexation. Barja and dos Santos Afonso (2005) described similar observations. Adsorbed HA shows two intense IR absorption
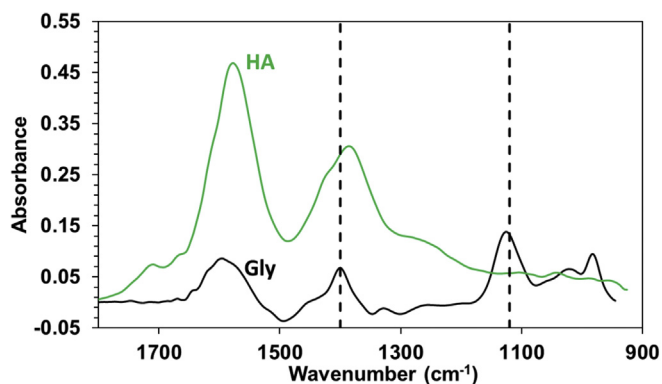
Fig. 2. ATR–FTIR spectra of adsorbed Gly ($\Gamma_{Gly} = 0.175$ mg m^{-2}) and adsorbed HA ($\Gamma_{HA} = 1.20$ mg m^{-2}) on goethite. Selected wavenumbers (1120 and 1400 cm^{-1}) for quantification are shown by the vertical dashed lines.

bands at 1575 and 1385 cm^{-1}, a broad shoulder at 1065 cm^{-1} and two weak bands at 1105 and 1047 cm^{-1}. The two intense bands at 1575 and 1385 cm^{-1} are characteristic of carboxylate (COO$^-$) groups, $\nu_a(C-O)$ and $\nu_s(C-O)$ vibration modes, respectively, whereas the shoulder was attributed to carboxylic (COOH) groups and the two weak bands to polysaccharide-like moieties (Lumsdon and Fraser, 2005; Kang and Xing, 2008).

The selected wavenumbers to quantify Γ_{HA} and Γ_{Gly} with Eqs. (2) and (3) were 1400 and 1120 cm^{-1}. Even though the stronger IR absorption of HA occurs at 1575 cm^{-1}, the 1400 cm^{-1} wavenumber was preferred because of the mentioned spectral artifacts that water generates close to 1600 cm^{-1}. The 1120 cm^{-1} wavenumber was selected because Gly has an important absorption at 1120 cm^{-1}, whereas the absorption of HA is weak. Absorbance vs Γ_{HA} plots at both selected wavenumbers were linear (see Supplementary material, Fig. S1). The linearity of Absorbance vs Γ_{Gly} plots was already demonstrated in a previous publication (Waiman et al., 2013). From these plots, the following κ values were determined in order to solve Eqs. (2) and (3): $\kappa_{HA}^{1120} = 0.0487$ m^2 mg^{-1}, $\kappa_{HA}^{1400} = 0.259$ m^2 mg^{-1}, $\kappa_{Gly}^{1120} = 0.664$ m^2 mg^{-1} and $\kappa_{Gly}^{1400} = 0.249$ m^2 mg^{-1}.

3.2.1. Gly adsorption on HA-containing goethite

Fig. 3 shows the evolution of the ATR-FTIR spectra of goethite samples subjected first to adsorption of HA to achieve the different surface loading of 0.32, 0.62 and 1.25 mg m^{-2}, followed by the addition of a 16.9 mg L^{-1} Gly solution. Since all these experiments started with the addition of HA, there was only HA adsorption at the beginning, which is shown by the green spectra in the figure. In the case of Fig. 3A green spectra due to adsorbed HA grow with time, and the last spectrum corresponds to the desired loading of $\Gamma_{HA} = 0.32$ mg m^{-2}. The replacement of the solution in contact with the goethite film by the Gly solution produces the appearing of the IR bands of adsorbed Gly. Bands in the $950-1170$ cm^{-1} region are well detected, and the presence of the Gly bands at around 1400 cm^{-1} and 1585 cm^{-1} mounted on the respective HA bands is also evident. The results show that Gly adsorbs on this HA-containing goethite sample. Fig. 3B is the case where HA was added to attain an intermediate loading of $\Gamma_{HA} = 0.62$ mg m^{-2}. The subsequent addition of Gly produces changes in the spectra due to Gly adsorption. However, these changes are smaller than in Fig. 3A as the result of a lower adsorption of Gly. The last case is shown in Fig. 3C, where HA was added to attain a loading of $\Gamma_{HA} = 1.25$ mg m^{-2}, aiming to completely saturate the goethite surface with HA. This was done by replacing several times the HA solution in contact with the goethite film with new HA solutions. The spectra recorded after the addition of Gly were nearly coincident with the last spectrum of adsorbed HA, showing that under this condition the adsorption of Gly was very limited.

Calculated Γ_{HA} and Γ_{Gly} as a function of time after Gly addition are shown in Fig. 4A and B respectively. For the case of Gly, Γ_{Gly} data obtained under the same conditions but with a HA loading $\Gamma_{HA} = 0$ mg g^{-1} (Gly adsorption on bare goethite surface) are included for comparison. Fig. 4A shows that the addition of Gly does not produce any change in HA adsorption. Γ_{HA} vs. t curves remain flat for the three investigated HA loadings, indicating that HA is strongly bonded to goethite and that cannot be displaced by Gly, facts that were already noticed with adsorption isotherms. On the contrary, Fig. 4B shows that the presence of HA at the goethite surface affects significantly Gly adsorption, decreasing the Gly adsorption rate as the HA loading increases. The effects of increasing HA can be well understood in terms of a decreasing availability of surface sites and an increasing electrostatic repulsion between adsorbed HA and adsorbing Gly. The only information found in the literature regarding glyphosate adsorption kinetics on
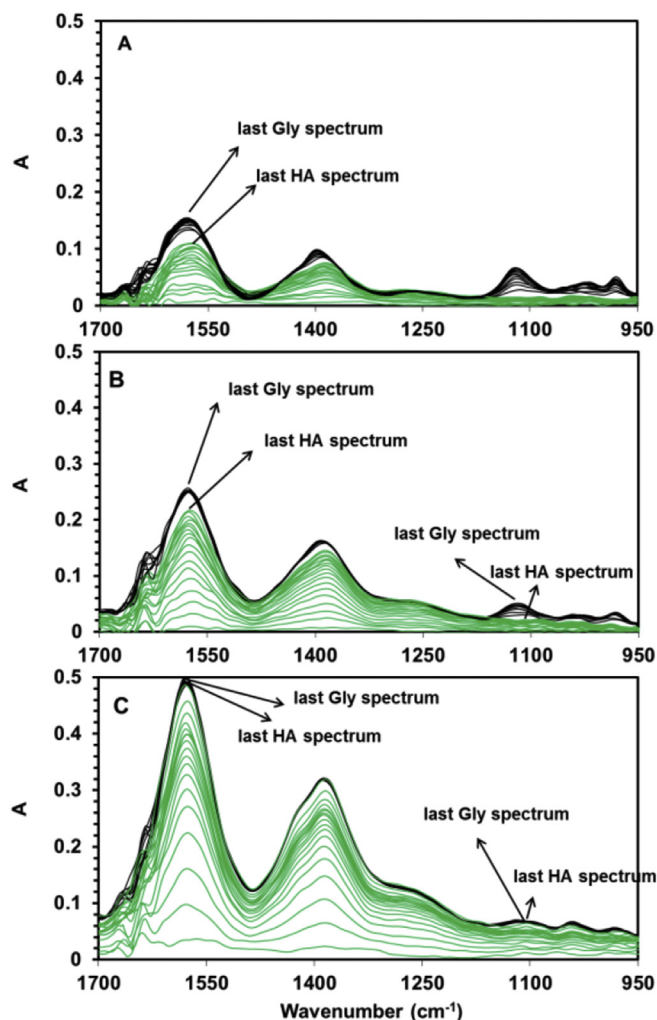
Fig. 3. ATR-FTIR spectral evolution in time in experiments where HA was adsorbed first (green spectra) followed by the addition of a 16.9 mg L^{-1} (10^{-4} M) Gly solution (black spectra). The value of Γ_{HA} before Gly addition was A) 0.32, B) 0.62 and C) 1.25 mg m^{-2}. Only one out of two recorded spectra are shown. Shown spectra were recorded every 6 min. Overall time taken to record all spectra for HA adsorption was 120 min, and for Gly adsorption was 24 min. (For interpretation of the references to color in this figure legend, the reader is referred to the web version of this article.)
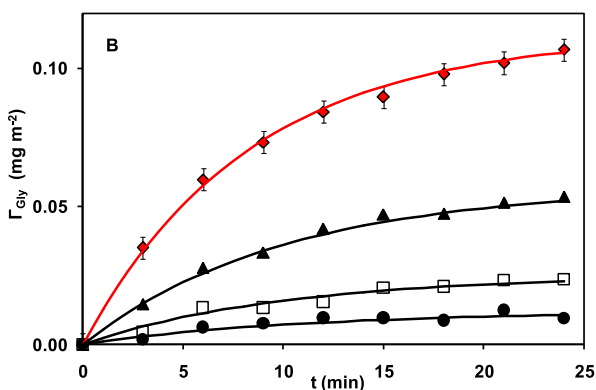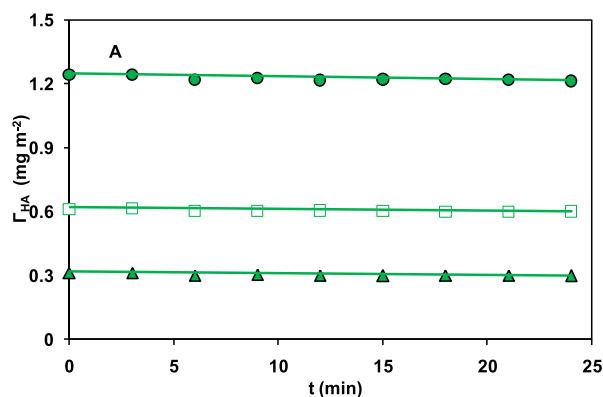
HA-coated goethite or other HA-coated solid was one experiment performed by Day et al. (1997) showing that Gly adsorption on a HA-coated goethite was considerably slower than on pure goethite, in line with the results of Fig. 5.

3.2.2. Gly desorption by addition of HA

Fig. 5A—C show the effects of adding HA to a goethite sample that previously contained adsorbed Gly. The adsorption of Gly is shown by the black spectra, which are very similar in the three cases because the Gly concentration was always the same. The replacement of the solution in contact with the goethite film by the 233 mg L^{-1} HA solution (Fig. 5A) produces an increase in the absorbance in the spectral region above 1200 cm^{-1}, indicating that HA adsorbs on goethite. The visual inspection of the spectra in this region does not allow to detect if there is some Gly desorption accompanying the HA adsorption. This doubt can be solved by inspecting the spectral region below 1200 cm^{-1}, where the absorbance of HA is lower than that of Gly. At around 1120 cm^{-1}, for example, there is a small but detectable decrease in absorbance after HA was added. This is a good indication of Gly desorption accompanying HA adsorption. Otherwise, the absorbance at around 1120 cm^{-1} would have increased after HA addition. Fig. 5B and C show the results of analogous experiments, but with lower HA concentrations: 116 and 50 mg L^{-1}, respectively. There is HA adsorption accompanied by Gly desorption in both cases. A simple inspection to the spectra in Fig. 5A—C indicates that HA adsorption increases as the HA concentration increases. It is not so straightforward, however, to deduce how HA concentration affects Gly desorption, and thus calculations using Eqs. (2) and (3) need to be analyzed.

Calculated Γ_{HA} and Γ_{Gly} as a function of time after HA addition are shown in Fig. 6A and B respectively. For the case of Gly, Γ_{Gly} data obtained under the same conditions but with a HA concentration of 0 mg L^{-1} (just washing with 0.1 M NaCl, pH 7.0) are also included for comparison. Fig. 6A confirms that HA adsorbs in all cases and that adsorption increases by increasing HA concentration. Fig. 6B, on the other hand, shows that increasing the HA concentration increases the desorption rate of Gly. There is no data in the literature to compare with data presented here.

3.2.3. A rate law for Gly desorption

Kinetic studies at surfaces are useful to understand reaction mechanisms (Sparks, 1989) and in practical situations where sur-
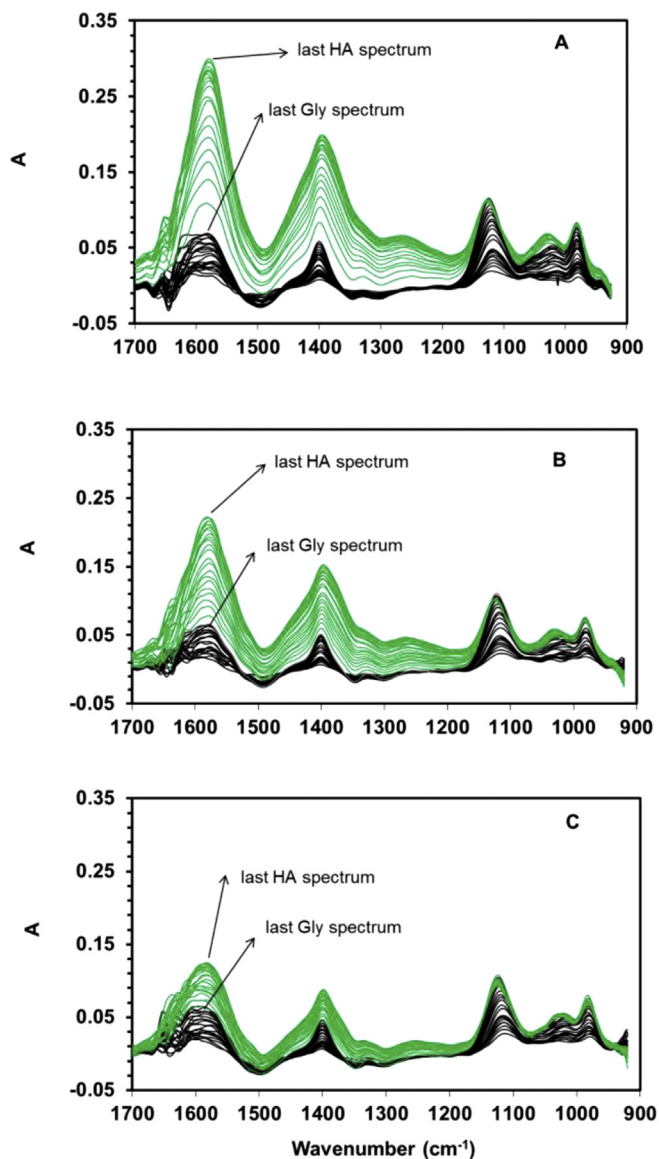

Fig. 4. A) Γ_{HA} vs. t and B) Γ_{Gly} vs. t curves after the addition of a 16.9 mg L^{-1} (10^{-4} M) Gly solution to HA-containing goethite with: (diamonds) $\Gamma_{HA} = 0$ mg m^{-2}, (triangles) $\Gamma_{HA} = 0.32$ mg m^{-2}, (squares) $\Gamma_{HA} = 0.62$ mg m^{-2}, (circles) $\Gamma_{HA} = 1.25$ mg m^{-2}. Data corresponds to spectra of Fig. 3. Error bars are standard deviations and are shown for one curve (See Supplementary material).

Fig. 5. ATR-FTIR spectral evolution in experiments where Gly was adsorbed first (black spectra) by adding a 16.9 mg L^{-1} (10^{-4} M) Gly solution, followed by the addition of HA solutions (green spectra) of three different concentrations: A) 233 mg L^{-1}, B) 116 mg L^{-1}, C) 50 mg L^{-1}. Shown spectra were recorded every 3 min. (For interpretation of the references to color in this figure legend, the reader is referred to the web version of this article.)

dependency can be observed, indicating that Gly desorption is also first order in adsorbed Gly. Therefore, results in Fig. 7 allow establishing the following experimental rate law for desorption of Gly in the presence of HA:

$$R_d = k_{d,0} \Gamma_{Gly} + k_{d,HA} \Gamma_{Gly} c_{HA} \tag{4}$$

where R_d is the initial desorption rate of Gly, $k_{d,0}$ is the rate constant for desorption of Gly in absence of HA and $k_{d,HA}$ is the rate constant for desorption of Gly caused by HA. The term $k_{d,0}\Gamma_{Gly}$ is directly the y-axis intercept of the straight line in Fig. 7A, whereas the product $k_{d,HA}\Gamma_{Gly}$ is its slope. From these data the values for $k_{d,0} = 3.1 \times 10^{-3}$ min^{-1} and $k_{d,HA} = 2.1 \times 10^{-5}$ L mg^{-1} min^{-1} were calculated.

Eq. (4) indicates that the initial desorption rate of Gly is the sum of two parallel desorption processes: i) a direct desorption of Gly by the electrolyte, process that is first order in adsorbed Gly and is represented by the first term of the right-hand-side of the equation, and ii) a desorption assisted by HA, first order in adsorbed Gly and first order in dissolved HA, represented by the second term of the right-hand-side of the equation. Therefore, the results can be understood in terms of the following kinetic processes:

$$\equiv SGly \xrightarrow{k_{d,0}} \equiv S + Gly \tag{5}$$

$$\equiv SGly + HA \xrightarrow{k_{d,HA}} \equiv SHA + Gly \tag{6}$$
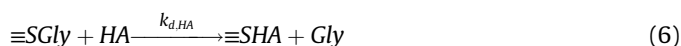
where $\equiv S$ represents a surface site at the goethite surface, $\equiv SGly$ is adsorbed Gly and $\equiv SHA$ is adsorbed HA. Reaction (5) accounts for a direct Gly desorption in absence of HA, and gives the first order dependency in adsorbed Gly. Reaction (6) is Gly desorption caused by ligand exchange with HA, giving the first order dependency in adsorbed Gly and dissolved HA. It is probable that the direct Gly desorption in absence of HA is also a ligand exchange, where the leaving ligand (Gly) is substituted by a water molecule, or even a chloride ion from the electrolyte, which act as the incoming ligands. The measured rate constants for both processes lead to a half-life of 3.7 h for the first process, and to a half-life of 1.4 h for the second process in a 400 mg L^{-1} HA solution. For HA concentrations lower than 150 mg L^{-1}, the half-life of the process becomes longer than 3.7 h and thus direct detachment from the surface prevails. However, in soil remediation processes, where solutions obtained from composts and having dissolved organic carbon (DOC) concentrations of around 1500 mg L^{-1} or higher are applied (Chiang et al., 2016), the controlling process will be surely the second one.

4. Conclusions

The effects of HA on the adsorption–desorption of Gly on goethite were investigated under pseudo equilibrium conditions by adsorption isotherms and under kinetic conditions by ATR-FTIR spectroscopy. Adsorption isotherms reveal that the presence of HA decreases the adsorption of Gly as a consequence of HA adsorption. The adsorption is almost completely impeded when the goethite surface is saturated with adsorbed HA molecules. The opposite effect was not observed: HA adsorption was not affected by the presence of Gly under the studied conditions, because HA binds stronger than Gly the goethite surface.

The use of ATR-FTIR spectroscopy made possible the simultaneous quantification of adsorbed Gly and HA on goethite, and to study the effects of HA on the adsorption/desorption kinetics of Gly. Since the shape of Gly spectra does not change during Gly adsorption or desorption, it can be concluded that always the same inner-sphere surface complex is involved in the processes. HA

face reactions rates need to be known (Azizian, 2004). In order to have some insights into the mechanism of Gly desorption from goethite, kinetic data were analyzed to obtain a rate law, where the reaction rate is expressed in terms of the concentration of reactants.
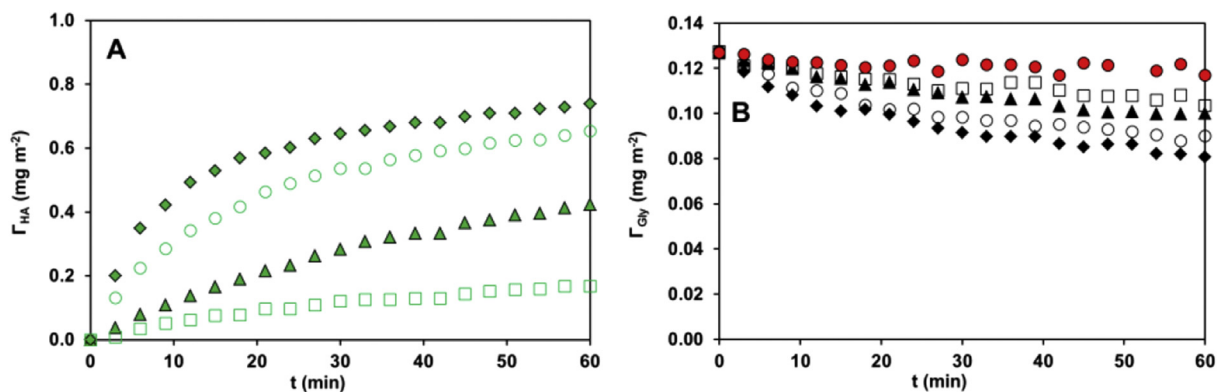
Initial desorption rates of Gly were quantified from the initial slopes of the curves in Fig. 6B, and are plotted as a function of HA concentration in Fig. 7A. The desorption rate increases linearly with HA concentration, indicating that Gly desorption is first order in dissolved HA. The straight line has a non-zero y-axis intercept, meaning that in absence of HA (c$_{HA}$ = 0) the pure electrolyte can desorb Gly from goethite at a measurable rate. The desorption rate should also vary with the amount of adsorbed Gly, therefore three desorption experiments (see Supplementary material, Fig. S2) were performed in order to evaluate how the desorption rate depends on Γ_{Gly}. The rate vs. Γ_{Gly} plot is shown in Fig. 7B, where a linear

Fig. 6. (A) HA adsorption and (B) the corresponding Gly desorption curves. Adsorbed Gly was the same at the beginning of all experiments (0.127 mg m^{-2}), and c_{HA} was varied: (solid circle) 0, (squares) 50, (triangles) 116, (open circles) 233 and (diamonds) 466 mg L^{-1}.
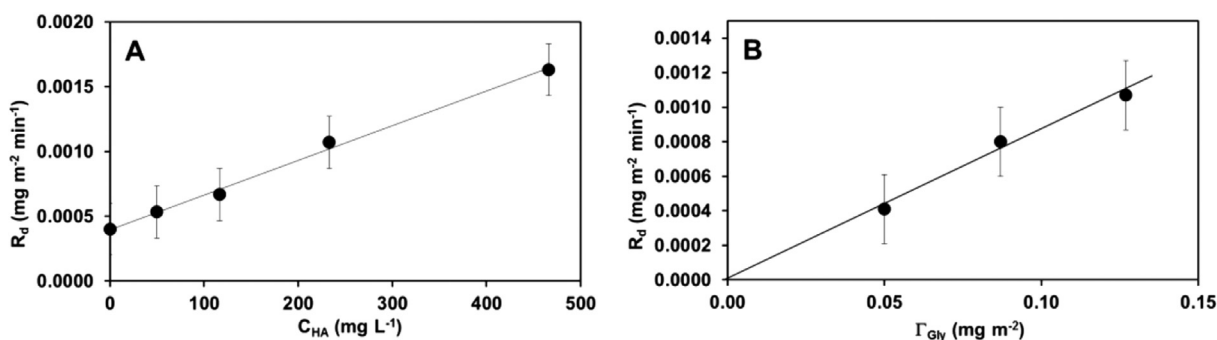

Fig. 7. (A) Effect of c_{HA} on the Gly desorption rate with Γ_{Gly} = 0.127 mg m^{-2}, as obtained from data in Fig. 6B. (B) Effect of Γ_{Gly} on the Gly desorption rate using c_{HA} = 233 mg L^{-1}.

affects both, the adsorption and the desorption rates of Gly. The presence of HA at the surface decreases significantly the adsorption rate because adsorbed HA blocks reactive sites at the goethite surface and probably because an electrostatic repulsion between adsorbed HA and adsorbing Gly. Regarding desorption kinetics, data suggests that adsorbed Gly is desorbed by two parallel processes: direct detachment from the surface, as indicated by reaction (5), and ligand exchange with HA, as indicated by reaction (6). The general findings have important environmental implications. The first one is that the presence of humic substances in soils decreases both, the adsorbed amount and the adsorption rate of Gly because Fe (hydr)oxides and Al (hyd)oxides, which should be the main Gly adsorbent by ligand exchange, will have their surface significantly occupied with organic matter. In addition, if Gly is adsorbed on metal oxides in soils, any process that increases the dissolution of humic substances (such as an increase in pH) will significantly increase the desorption rate of Gly. This second implication will become very important when using remediation technologies, where solutions highly concentrated in DOC are applied to soils. In all cases, the environmental mobility of Gly will be increased.

The combination of adsorption isotherms and ATR-FTIR spectroscopy gives useful equilibrium and kinetic information on the effects of HA on the adsorption–desorption behavior of Gly. Rate constants for Gly desorption were quantified and half-lives for adsorbed Gly were estimated, which are important parameters to understand the effects of the goethite surface in the mobility and fate of Gly in the environment.

Appendix A. Supplementary material

Supplementary material related to this article can be found at http://dx.doi.org/10.1016/j.chemosphere.2015.11.082.

References

Antelo, J., Arce, F., Avena, M., Fiol, S., López, R., Macías, F., 2007. Geoderma 138, 12–19.
Aparicio, V.C., De Gerónimo, E., Marino, D., Primost, J., Carriquiriborde, P., Costa, J.L., 2013. Chemosphere 93, 1866–1873.
Atkinson, R.J., Posner, A.M., Quirk, J.P., 1967. J. Phys. Chem. 71, 550–558.
Azizian, S., 2004. J. Colloid Interface Sci. 276, 47–52.
Barja, B.C., dos Santos Afonso, M., 2005. Environ. Sci. Technol. 39, 585–592.
Candela, L., Caballero, J., Ronen, D., 2010. Sci. Total Environ. 408, 2509–2516.
Celis, R., Hermosin, M.C., Cox, L., Cornejo, J., 1999. Environ. Sci. Technol. 33, 1200–1206.
Chiang, P.N., Tong, O.Y., Chiou, C.S., Lin, Y.A., Wang, M.K., Liu, C.C., 2016. J. Hazard. Mater. 301, 100–105.
Day, G.M., Hart, B.T., McKelvie, I.D., Beckett, R., 1997. Environ. Technol. 18, 781–794.
Fu, H.B., Quan, X., 2006. Chemosphere 63, 403–410.
Gimsing, A.L., Borggaard, O.K., 2001. Clays Clay Miner. 49, 270–275.
Gimsing, A.L., Borggaard, O.K., 2002. Clay Miner. 37, 509–515.
Guytona, K.Z., Loomis, D., Grosse, Y., El Ghissassi, F., Benbrahim-Tallaa, L., Guha, N., Scoccianti, C., Mattock, H., Straif, K., 2015. Lancet 16, 490–491.
Kang, S., Xing, B., 2008. Langmuir 24, 2525–2531.
Lumsdon, D.G., Fraser, A.R., 2005. Environ. Sci. Technol. 39, 6624–6631.
Ma, J., Li, X., 2015. Chemosphere 128, 293–298.
Puccia, V., Luengo, C., Avena, M., 2009. Colloids Surf. A 348, 221–227.
Roncaroli, F., Blesa, M.A., 2011. J. Colloid Interface Sci. 356, 227–233.
Sheals, J., Sjöberg, S., Persson, P., 2002. Environ. Sci. Technol. 36, 3090–3095.
Sola, N.H., Ceppi, S.B., Sereno, R., 1988. Cienc. del Suelo 6, 108–112 (published in Spanish).

Sparks, D.L., 1989. Kinetics of Soil Chemical Processes. Academic Press, San Diego.

Swift, R.S., 1996. Organic matter characterization. In: Sparks, D.L. (Ed.), Methods of Soil Analysis. Part 3. Chemical Methods, SSSA Book Series: 5. WI, USA, pp. 1011–1069.

Tipping, E., 1994. Comput. Geosci. 20, 973–1023.

Waiman, C.V., Avena, M.J., Garrido, M., Fernández Band, B., Zanini, G.P., 2012. Geoderma 170, 154–158.

Waiman, C.V., Avena, M.J., Regazzoni, A.E., Zanini, G.P., 2013. J. Colloid Interface Sci. 394, 485–489.

Weng, L., Van Riemsdijk, W.H., Koopal, L.K., Hiemstra, T., 2006. J. Colloid Interface Sci. 302, 442–457.

Yang, X., Wang, F., Bento, C.P.M., Xue, S., Gai, L., van Dam, R., Mol, H., Ritsema, C.J., Geissen, V., 2015. Sci. Total Environ. 512–513, 406–414.